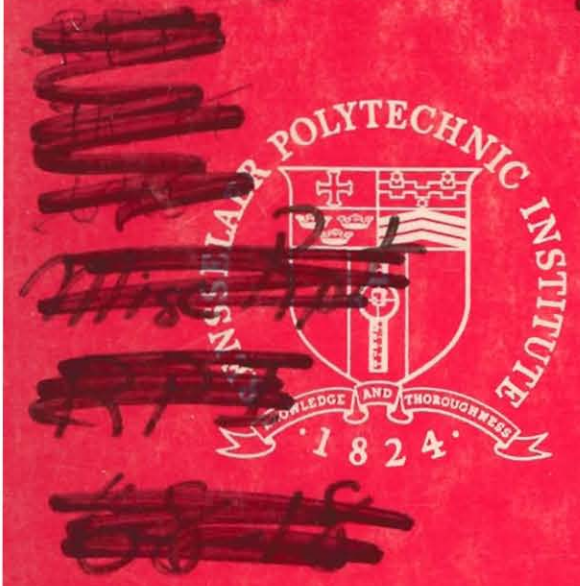

PROJECT TUBEFLIGHT

C. C. SUN

RECIRCULATORY FLOW IN PERIPHERAL–JET SUPPORTS

TR PT 6805

RECIRCULATORY FLOW IN PERIPHERAL-JET SUPPORTS

by
Chen-C. Sun

This research was supported by the National Science Foundation under Grant No. GK-618.

RENSSELAER POLYTECHNIC INSTITUTE
TROY, NEW YORK

June, 1968

ACKNOWLEDGMENT

The author wishes to express his appreciation and gratitude to Dr. Thomas J. Black for his guidance and continued encouragement throughout the course of this work.

LIST OF SYMBOLS

b = constant

C_{p_i} = $\frac{p_c - p_a}{\frac{1}{2}\rho U_o^2}$

C_p = $\frac{p_c - p_a}{p_o - p_a}$

H = altitude of nozzle

J = momentum of jet

k = $\frac{\rho}{\chi_1}$

pa = atmospheric pressure

pc = cusshion pressure

po = total jet pressure

R = radius of curvature

r^* = dimensionless radius

t = width of nozzle exit

U_o = mean exit velocity of jet

V_θ = tangential velocity

V_r = velocity of radial direction

y^* = $r^* - 1$

ε = eddy viscosity

ρ = density of air

η = dimensionless variable = $k y^* \theta^{-\frac{3}{2}}$

ϕ_1 = inclination of nozzle

ϕ_2 = angle of jet impinges on the ground

ψ^* = stream function = $\theta^{\frac{1}{2}} f(\eta)$

χ_1 = constant of eddy viscosity

σ = $\frac{1}{2\sqrt{\chi_1 \lambda}}$

λ = $\frac{U_1 - U_2}{U_1 + U_2} = 1$

INTRODUCTION

One type of ground effect machine is designed so that the pressure of the air cushion is contained by a peripheral curtain jet. Analyses of this curtain, under the assumption of inviscid and incompressible flow, have been given by Ehrich[1] and Strand[2]. However, as first indicated by Chaplin[3], the effect of jet entrainment on the annular jet due to the viscosity of fluid flow is to reduce the cushion pressure significantly. Theories concerning the effect of mixing have been developed by Chaplin[3] and Bradbury[4]. Bradbury attempted to calculate the entrainment rate by approximating the curtain velocity distribution to that in a two-dimensional free jet[5].

Bradbury's analysis, however, is open to criticism on several grounds. In the first place it neglects the effect of the vortices which are established at both the inner and outer sides of the curtain jet, as discussed by Poisson-Quinton.[6] Secondly, the assumption that the turbulent mixing process in a curved jet is substantially the same as that in a straight jet is questionable. Experimental studies of jet flows in recent years (e.g. Grant[7]) suggests that the process of entrainment is controlled by coherent, transverse, high velocity eruptions of fluid from the jet centerline outwards, interspersed by regions of relatively slow inflow towards the centerline. It might therefore be argued that high curvature of the jet would selectively enhance these eruptive motion on the outer (convex) boundary of the jet and suppress them on the inner (concave) side. Consequently, in the case of the curtain jet, increased entrainment might be expected inside the curtain and decreased entrainment outside it. Finally, as discussed in more detail later, the horizontal momentum balance across the curtain is to some extent dependent on the slope of the velocity distribution immediately prior to impact of the jet curtain on the ground. Consequently it is important to determine the nature of this profile with some accuracy.

A major object of the present study is therefore to derive a more detailed analysis of the mixing process in a highly curved jet curtain and hence to obtain a more accurate estimate of the loss of cushion pressure due to jet mixing. A second objective is to determine the extent to which the cushion pressure is affected by the nature of the recirculative flow within the cushion. The present report presents preliminary attempts to establish a suitable mixing theory for the jet curtain.

DISCUSSION

1. Basic Equations of Motion

The annular jet is assumed to be two-dimensional at the moderate height/jet width ratios considered. The flow pattern is assumed to be as shown in Fig. 2. The jet is assumed to have constant curvature R until it impinges on the ground at an agle Φ_2 . Following impingement, a part (M_2) of the jet flows inward into the base cavity and the rest M_1 flows outward along the ground. In steady flow the inward mass flow M_2 must be equal to the mass entrainment from the base cavity. Since the velocity of the jet is not very high. The variation of the density of the flow is not appreciable, and the assumption of incompressible fluid is valid. The mixing process is assumed to be turbulent and government by an eddy viscosity .

The height/width of jet ratios (h/t) of practical interest here are in the range 3 - 6, so that the jet width t may be assumed small in relation to the radius of curvature, R, without incurring serious error. With this assumption, the relevant equation of motion and continuity may be written as[8]

$$\left(\frac{\partial V_r}{\partial r}\right) + \left(\frac{V_r}{r}\right) + \frac{1}{r}\left(\frac{\partial V_\theta}{\partial \theta}\right) = 0 \qquad (1)$$

$$V_r\left(\frac{\partial V_\theta}{\partial r}\right) + \frac{V_\theta}{r}\left(\frac{\partial V_\theta}{\partial \theta}\right) = \frac{\varepsilon}{\rho}\left(\frac{\partial^2 V_\theta}{\partial r^2}\right) \qquad (2)$$

$$\rho\left(\frac{V_\theta^2}{r}\right) = \frac{\partial P}{\partial r} \qquad (3)$$

where V_θ , V_r , ρ and ε are tangential velocity component, radial velocity component, fluid density and the eddy viscosity respectively.

Non-dimensionalizing equation (2) as follows

$$V_r^* = \frac{V_r}{U_o} \quad , \qquad V_\theta^* = \frac{V_\theta}{U_o} \quad , \quad r^* = \frac{r}{R} \quad , \quad y = \frac{y}{R} = r^* - 1 \tag{4}$$

Equation (2) becomes

$$\frac{U_o^2}{R} V_r^* \frac{\partial V_\theta^*}{\partial r^*} + \frac{U_o^2}{R} \frac{V_\theta^*}{r^*} \left(\frac{\partial V_\theta^*}{\partial \theta}\right) = \frac{\varepsilon}{\rho} \frac{R\theta U_o^2}{R^2} \left(\frac{\partial^2 V_\theta^*}{\partial r^{*2}}\right) \tag{5}$$

which gives

$$V_r^* \frac{\partial V_\theta^*}{\partial r^*} + \frac{V_\theta^*}{r^*} \left(\frac{\partial V_\theta^*}{\partial \theta}\right) = \frac{\varepsilon}{\rho} \theta \left(\frac{\partial^2 V_\theta^*}{\partial r^*}\right) \tag{6}$$

Now let $$\frac{\varepsilon_1}{\rho} = \frac{1}{k} \tag{7}$$

so that

$$V_r^* \frac{\partial V_\theta^*}{\partial r^*} + \frac{V_\theta^*}{r^*} \left(\frac{\partial V_\theta^*}{\partial \theta}\right) = \frac{\theta}{k} \left(\frac{\partial^2 V_\theta^*}{\partial r^{*2}}\right) \tag{8}$$

and equation (1) becomes

$$\frac{\partial V_r^*}{\partial r^*} + \frac{V_r^*}{r^*} + \frac{1}{r^*} \left(\frac{\partial V_\theta^*}{\partial \theta}\right) = 0 \tag{9}$$

The continuity equation (1) can be satisfied by a dimensionless stream function $\psi^* \left(= \frac{\psi}{U_o R}\right)$ such that

$$V_r^* = \left(-\frac{1}{r^*}\right) \left(\frac{\partial \psi^*}{\partial \theta}\right) \tag{10}$$

$$V_\theta^* = \frac{\partial \psi^*}{\partial r^*} \tag{11}$$

Assuming similarity variables

$$\eta = k\, y^*\, \theta^{b-2} \tag{12}$$

$$\psi^* = \theta^b f(\eta) \tag{13}$$

We obtain

$$V_r^* = -\frac{1}{r^*}\frac{\partial \psi^*}{\partial \theta} = -\frac{1}{r^*}\left[\theta^b f'(\eta)(b-2)\theta^{b-3} k y^* + b\theta^{b-1} f(\eta)\right]$$

$$\cong -\left[k(b-2)\theta^{2b-3} y^* f'(\eta) + b\theta^{b-1} f(\eta)\right] \tag{14}$$

$$V_\theta^* = \frac{\partial \psi}{\partial r^*} = \theta^b f(\eta) k\,\theta^{b-2} = k\,\theta^{2b-2} f'(\eta) \tag{15}$$

so that

$$\frac{\partial V_\theta^*}{\partial r^*} = k^2 \theta^{3b-4} f''(\eta) \tag{16}$$

$$\frac{\partial^2 V_\theta^*}{\partial \theta} = k^3 \theta^{4b-6} f'''(\eta) \tag{17}$$

and

$$\frac{\partial V_\theta^*}{\partial \theta} = (2b-2) k \theta^{2b-3} f'(\eta) + \theta^{4b-5} k^2 y^* (b-2) f''(\eta) \tag{18}$$

Substituting equations (14), (15), (16), (17) and (18) into equation (8) and using the approximation $r^* \cong 1$ we obtain

$$-\left[\theta^{2b-3} k y^* (b-2) f'(\eta) + b\theta^{b-1} f(\eta)\right]\theta^{3b-4} k^2 f''(\eta)$$

$$+ \theta^{2b-2} k f''(\eta)\left[(2b-2)\,\theta^{2b-2} k f'(\eta) + k^2 \theta^{2b-3} y^* (b-2)\theta^{b-3} f''(\eta)\right]$$

$$= \frac{1}{k} k^3 \theta\, \theta^{3b-6} f''(\eta) \tag{19}$$

$$k^2 \theta^{4b-5}\left[f''(\eta) + b f(\eta) f''(\eta) - (2b-2) f'^2(\eta)\right] = 0$$

$$f'''(\eta) + b f(\eta) f''(\eta) + (2-2b) f'(\eta) = 0 \tag{20}$$

Equation (20) with the appropriate boundary conditions provides the required description of the curved jet mixing region.

2. Preliminary Approximation Solution of Jet Mixing Process

As discussed later in Section 4 a major objective of the present program is to obtain an appropriate solution to the equation (20) and hence describe in detail, the process of entrainment and resultant decrease in effectiveness of the curved jet curtain. Before attempting this analysis, however, a preliminary approximate solution of the problem has been sought on the basis of a related analysis by Parks and Petersen[9] for the curved laminar wall jet. As will be seen, the mixing process in the wall jet flow has certain features in common with that in the curved jet curtain so that Petersen's tabulated solution of the former flow provides a quick and convenient first-step approach to the present problem.

The flow geometry for the case of the wall jet is shown in Fig. 2. The flow is initiated in essentially the same way as that in the jet curtain, i.e., by a two-dimensional jet of width t and uniform velocity U_o . This jet subsequently flows around a curved, convex solid surface of radius R and develops a characteristic profile as shown in which the velocity increases steadily from zero at the wall to a maximum some distance, $y = y_1$ (say) from the wall, and subsequently decreases to zero with further increase in y.

Since we may reasonably assume that the mixing process in the region $y \geq y_1$ is essentially similar to the mixing region on the convex side of the jet curtain, we may utilize that part of the wall jet solution for $y \geq y_1$ to describe the process of mixing and entrainment in the jet curtain. Two difficulties arise here: First, Petersen's analysis is for laminar flow and must be suitably modified for the present application in which turbulent flow is assumed; secondly, a problem arises in relation to the inner boundary conditions chosen, as will now be discussed.

In the case of the wall jet, the maximum velocity (which occurs at $y = y_1$) decreases steadily with distance along the curved path of the jet. In the case of the jet curtain, the situation is more complex. For small h/t ratios, the two mixing regions (on the inner and outer surfaces of the jet) will evidently not meet before the jet impinges on the wall (Fig. 7). The final jet profile immediately before impact will therefore comprise a central unmixed core region with a mixing type profile on either side of it. In this case the solution for each mixing region must satisfy the condition of constant maximum velocity where it bounds the core region.

For large h/t ratios, however, the mixing regions will evidently meet before the jet strikes the ground (Fig. 8) so that a fully-developed profile is obtained at a certain point, beyond which the maximum velocity in the jet will steadily decrease. We therefore utilize the wall-jet mixing solution with the understanding that the results obtained will probably not hold generally over a wide h/t range. Specifically we may expect the solution to fail at both the low and the high end of the h/t ratio range.

We accordingly seek a solution first for the turbulent wall-jet with the appropriate wall-jet boundary conditions.

$$\lim_{y^* \to \infty} V_\theta^* = 0 \quad \Rightarrow \quad f'(\infty) = 0 \tag{21}$$

$$\lim_{y^* \to \infty} \frac{\partial V_\theta}{\partial r} = 0 \quad \Rightarrow \quad f''(\infty) = 0 \tag{22}$$

$$\psi^* \big|_{y=0} = 0 \quad \Rightarrow \quad f(0) = 0 \tag{23}$$

$$V_\theta^* \big|_{y=0} = 0 \quad \Rightarrow \quad f'(0) = 0 \tag{24}$$

Integrating equation (20) from to we get

$$-f''(\eta) - b f(\eta) f'(\eta) + (2-3b) \int_\eta^\infty f'^2 d\eta = 0 \tag{25}$$

$\eta \geq 0 \qquad f'^2(\eta) \geq 0$

Let $h(\eta) = \int_\eta^\infty f'^2(\eta)\, d\eta$

we have $h(\eta) \geq 0$

Multiplying (25) by $f'(\eta)$ we get

$$-f'(\eta) f''(\eta) - b f(\eta) f'^2(\eta) + (2-3b) f'(\eta) h(\eta) = 0 \tag{26}$$

Again integrate (26) from η to ∞ yields

$$\tfrac{1}{2} f'^2(\eta) - b f(\eta) \int_\eta^\infty f'^2(\eta)\, d\eta + (2-4b) \int_\eta^\infty f'(\eta) h(\eta)\, d\eta = 0 \tag{27}$$

Evaluating equation (27) at η = 0 results in

$$(2-4b) \int_0^\infty f'(\eta) h(\eta)\, d\eta = 0 \tag{28}$$

Since $f'(\eta) \geq 0$, $h(\eta) > 0$ then $\int_0^\infty f'(\eta) h(\eta)\, d\eta \neq 0$

We therefore require that

$$2 - 4b = 0 \tag{29}$$

$$b = \tfrac{1}{2} \tag{30}$$

By (30), (12), (13), (15), (20) become

$$\eta = k y^* \theta^{-\frac{3}{4}} \tag{31}$$

$$\psi^* = \theta^{\frac{1}{2}} f(\eta) \tag{32}$$

$$V_\theta^* = \theta^{-1} k f'(\eta) \tag{33}$$

$$f'''(\eta) + \tfrac{1}{2} f(\eta) f''(\eta) + f'^2(\eta) = 0 \tag{34}$$

Let $f(\eta) = \tfrac{1}{2} g(\eta)$ equation (34) becomes

$$\tfrac{1}{2} g'''(\eta) + \tfrac{1}{8} g''(\eta) g(\eta) + \tfrac{1}{4} g'^2(\eta) = 0 \tag{35}$$

boundary conditions

$$g(0) = 0, \quad g'(0) = 0, \quad g'(\infty) = 0, \quad g''(\infty) = 0 \tag{36}$$

Equation (35) with boundary conditions (36) has been solved by Parks and ersen[1] as follows:

$$g_\infty = \lim_{\eta \to \infty} g \tag{37}$$

F is a parameter between 0 and 1.

$$\eta = \frac{1}{g_\infty}\left\{4(3^{\frac{1}{2}})\arctan\left[\frac{F(3^{\frac{1}{2}})}{2+F}\right] + 2\ln\left[\frac{F^2+F+1}{(F-1)^2}\right]\right\} \tag{38}$$

$$g = g_\infty F^2 \tag{39}$$

$$g' = g_\infty^2 \frac{(F-F^4)}{6} \tag{40}$$

$$g'' = g^3\left(\frac{1}{72}\right)(1-F^3)(1-4F^3) \tag{41}$$

$$g''' = -g_\infty^4\left(\frac{1}{288}\right)F^2(1-F^3)(5-8F^3) \tag{42}$$

For g_∞ = 1.000 is of special importance and has been prepared by Parks Petersen[1] in Table I and Fig. 4.

We now wish to write only that part of the above solution which applies ide the point of maximum wall jet velocity $y \geq y_1$. Let η_1, y_1^* corres- to this point of maximum velocity and let θ_B be the turning angle of the curtain from nozzle exit to the point of impingement as shown in Fig. 2.

We now make the further assumption that the portion of the jet curtain next ne cavity, which is represented by the truncated wall jet solution, carries isely half the curtain jet momentum flux and half the curtain jet mass flow ne point of impingement on the ground. The first assumption implies 1/2 total nomentum

$$\frac{1}{2}\rho U_i^2 t = \left[\int_{y_1}^{\infty} \rho V_0^2 dy\right]_{\theta_B} = \frac{\rho U_i^2 R k^2 \theta_B^{-2}}{k\,\theta_B^{-\frac{1}{2}}}\left\{-2\left[f'(\eta) + \frac{1}{2}f(\eta)f'(\eta)\right]_{\eta_1}^{\infty}\right\} \tag{43}$$

This assumption would appear reasonable with the framework of the present preliminary analysis. Reorganizing (43), we obtain

$$\theta_B^{\frac{1}{2}} = 2k\left(\frac{R}{t}\right)\left\{2\left[f''(\eta_1) + \frac{1}{2}f'(\eta_1)f(\eta_1)\right]\right\} \tag{44}$$

But $f'(\eta_1)$ is maximum $f''(\eta_1) = 0$

$$\theta_B^{\frac{1}{2}} = 2k\left(\frac{R}{t}\right)\left[f'(\eta_1)\, f(\eta_1)\right] \tag{45}$$

Now let y_2, η_2 correspond to the divided stream line which divides the total mass flow in the jet curtain into m_1 which flow outwards and m_2 which flows back into the cavity. The second assumption above implies that

$$\begin{aligned}\frac{1}{2}\rho U_0 t = \int_{y_1}^{y_2}\rho V_\theta\, dy &= \frac{\theta_B^{3/2}\rho U_0 R}{k}\int_{\eta_1}^{\eta_2} k\theta_B^{-1} f'(\eta)\, d\eta \\ &= \frac{\rho U_0 R}{\theta_B^{-\frac{1}{2}}}\left[f(\eta_2) - f(\eta_1)\right]\end{aligned} \tag{46}$$

$$\theta_B^{-\frac{1}{2}} = 2\left(\frac{R}{t}\right)\left[f(\eta_2) - f(\eta_1)\right] \tag{47}$$

In the case of steady flow the entrained mass flow should be equal to the mass flow inward to the base cavity. As shown in Fig. 2

$$J_2 = \int_{y_2}^{\infty}\rho V_\theta^2\, dy\Big|_{\theta_B} = \rho U_0^2 k R\theta_B^{\frac{1}{2}}\left[2f''(\eta_2) + f(\eta_2)f'(\eta_2)\right] \tag{48}$$

$$\begin{aligned}J_1 &= \frac{1}{2}\rho U_0^2 t + \int_{\eta_1}^{\eta_2}\rho V_\theta^2\, dy \\ &= \frac{1}{2}\rho U_0^2 t - 2\rho U_0^2 k R\theta_B^{-\frac{1}{2}}\left[f''(\eta_2) + \frac{1}{2}f'(\eta_2)f(\eta_2)\right. \\ &\qquad \left. - f''(\eta_1) - \frac{1}{2}f(\eta_1)f'(\eta_1)\right]\end{aligned} \tag{49}$$

To find the angle of impingement, let us consider the control volume ABCD in Fig. 4. $\overline{AB}$, $\overline{CD}$ are small so we may neglect the pressure difference on surface $\overline{AB}$ and $\overline{CD}$. The momentum equation for the x-direction gives

$$J\cos\phi_2 = J_1 - J_2 \tag{50}$$

$$\rho U_0^2 t \cos\phi_2 = \frac{1}{2}\rho U_0^2 t + \rho U_0^2 k R \theta_B^{-\frac{1}{2}} [2f''(\eta_1) + f'(\eta_1) f(\eta_1) - 4f''(\eta_2) - 2f(\eta_2) f'(\eta_2)] \quad (51)$$

$$\cos\phi_2 = \frac{1}{2} + k\theta_B^{-\frac{1}{2}} \left(\frac{R}{t}\right) [2f''(\eta_1) + f'(\eta_1) f(\eta_1) + f''(\eta_2) - 2f(\eta_2) f'(\eta_2)] \quad (52)$$

Eliminate $k\theta_B^{-\frac{1}{2}}\left(\frac{R}{t}\right)$ in (52) by substituting equation (45) into (52)

$$\cos\phi_2 = \frac{1}{2} + \frac{1}{2} \frac{1}{f'(\eta_1) f(\eta_1)} [2f''(\eta_1) + f'(\eta_1) f(\eta_1) - 4f''(\eta_2) - 2f(\eta_2) f'(\eta_2)] \quad (53)$$

Geometric relationships (Fig. 3) give

$$\theta_B = \pi - \phi_1 - \phi_2 \quad (54)$$

$$H = R(\cos\phi_1 + \cos\phi_2) \quad (55)$$

$$\frac{H}{R} = \cos\phi_1 + \cos\phi_2 \quad (56)$$

The momentum equation of control volume ABCD in Fig. 2 gives

$$(P_c - P_a) H = J\cos\phi_1 + J_1 - J_2 = J(\cos\phi_1 + \cos\phi_2)$$

$$C_{p_1} = \frac{P_c - P_a}{\frac{1}{2}\rho U_0^2} = \frac{2J}{\rho U_0^2 H} [\cos\phi_1 + \cos\phi_2]$$

$$= 2\left(\frac{t}{H}\right)(\cos\phi_1 + \cos\phi_2) = 2\left(\frac{t}{R}\right) \quad (57)$$

We may now summarize and simplify the equations required to calculate the cushion pressure as a function of the variable involved. These equations are (45), (53), (54), (56), (57), and (58) as tabulated again below

Let $\lim_{\eta^* \to \infty} g_1(\eta^*) = 1.000$

$$\eta = \frac{\eta^*}{g_\infty} \qquad g = g_\infty g_1 \qquad g' = g_\infty^2 g_1' \qquad g'' = g^3 g_1''$$

$$\cos\phi_2 = \frac{1}{2}\left\{1 + \frac{1}{g_1(\eta_1^*)\,g_1'(\eta_1^*)}\left[4g_1''(\eta_1^*) + g_1'(\eta_1^*)\,g_1(\eta_1^*) - 8\,g_1''(\eta_2^*) - 2\,g_2(\eta_2^*)\,g'(\eta_2)\right]\right\}$$

$$g_\infty^2 = \frac{2\theta_B}{k} \times \frac{g_1(\eta_2^*) - g(\eta^*)}{g_1(\eta^*)\,g_1'(\eta_1^*)}$$

$$\frac{t}{k} = \theta_B^{\frac{1}{2}}\, g_{10}\left[g_1(\eta_2^*) - g_1(\eta_1^*)\right] \qquad (64)$$

$$\theta_B = \pi - \phi_1 - \phi_2$$

$$\frac{H}{t} = \frac{2(\cos\phi_1 + \cos\phi_2)}{C_{p_1}}$$

$$C_{p_1} = 2\left(\frac{t}{k}\right)$$

$$C_p = \frac{2C_{p_1}}{C_{p_1}+2}$$

Numerical Example

The use of equations (64) to calculate coefficient of pressure C_p can illustrated by the following example:

For the case of the nozzle exit angle $\phi_1 = 60^\circ$ choose the typical value $\sigma = 13.5^8$, $\rho = 0.00234$ lbm/ft^3 $\chi_1 = \frac{1}{4 \times 13.5^2}$. We then get

$k = \sqrt{\frac{\rho}{\chi_1}} = \sqrt{0.00234 \times 4 \times 13.5} = 1.31$, $F_1 = 0.6300$, $\eta_1^* = 8.114793$, $g_1(\eta_1^*) = 0.3969$, $g'(\eta_1^*) = 0.078745$ $g''(\eta_1^*) = 0$. Let η_2 be the coordinate of e dividing streamline. Let $F_2 = 0.85$, $\eta_2^* = 12.784859$. Substitute into (41) get

$$\cos\phi_2 = 0.735 \qquad C_{p_1} = 3.000 \qquad C_p = 1.200$$

Several calculations are made and the results are tabulated in Table 2 and ote in Fig. 8 in comparison with the result of inviscid theory and Ribich's sult.

As seen the present theory provides reasonable agreement with Ribich's[10] results over a range of moderate h/t ratios. The theoretical values are too high at low h/t, and too low at high h/t's. However, in view of the gross nature of the assumptions made in this preliminary attempt to obtain a solution, it is felt that the results are at least sufficiently encouraging to warrant further and more exact ana,ysis of the jet curtain mixing process along the present lines as proposed in section 4 which follows.

4. Extension of Present Study

Fig. 8 shows a good agreement between the preliminary approximate analysis and Ribich's result at moderately high height to thickness (h/t) ratio. However, when the height to thickness ratio (h/t) is small, the preliminary solution we have obtained deviates considerably from Ribich's results. This deviation is probably due to the fact that some of the assumptions made become increasingly suspect at low h/t ratio. When the height to thickness ratio is small, the mixing layers on both sides of the curtain jet do not meet before the point of impact on the ground. As shown in Figure 7 the jet can then be divided into three regions. These are (1) an inner shear layer, (2) an unmixed core, and (3) an outer shear layer. When the jet thickness is large, the assumption U_o = constant at nozzle exit may no longer be a good approximation, and $U_o \propto \frac{1}{r}$ (inviscid vortex) is probably a more desirable assumption. A more detailed and precise analysis of mixing and entrainment at low h/t is therefore necessary. Referring to Figure 7 the velocity profile in region 1 can be approximated by the velocity profile we have obtained in Section 2 while a similar treatment can be applied to the outer mixing region 3. The assumption of constant velocity, or , alternatively of inviscid vortical motion will be made in the core region, with the overall condition that jet momentum is conserved.

Similar to our preliminary analysis, we can then formulate equation at the point of impact to determine the amount of entrainment on the inside of curtain jet and hence the amount of recirculatory flow.

Another important objective that needs a careful consideration is the actual recirculatory flow within the cushion and the effect of energy losses in this region. The existence of vortices induced by the curtain make the pressure within it nonuniform[6] and the outside may also differ from the atmosphere value. The effect of external vortices will probably reduce the local pressure acting on the curtain and hence reduce the cushion pressure p_c. This effect will undoubtedly be accentuated by vehicle forware speed. No serious analytical study has yet been made of the effect of motion on cushion pressure and this problem will consequently be of primary interest also in the current study.

REFERENCES

1. Ehrich, F.F., "The Curtain Jet," JAS, November 1961.

2. Strand, T., "Exact Inviscid Incompressible Flow Theory of Static Peripheral Jet in Proximity to the Ground," Convair Division, General Dynamics Co., Engineering Research Report SD-002, November 1959.

3. Chaplin, H.R., "The Effect of Jet Mixing on the Annular Jet," David Taylor Model Basin, Report 1375, 1959.

4. Bradbury, L.J.S., "A Mixing Theory for the Hovering of Peripheral Jet Air Cushion Vehicles," R.A.S. Volume 71, January 1967.

5. Tollmien, W., "Calculation of Turbulent Expansion Process," NACA Tech. Memo 1085, (1945).

6. Poisson-Quinton," Two Dimensional Studies of a Ground Effect Plateform," Translated by D.C. Hagen, Dept. of Aeronautical Engineering, Princeton University.

7. Grant, H.L., "The Large Eddies of Turbulent Motion,"J. Fluid Mechanics, Volume 4, 1958.

8. Schlichting, H., "Boundary Layer Theory," McGraw Hill Book Co., Inc.

9. Parks, E.K., and Petersen, R.E., "Analysis of a Coanda Type Flow," AIAA Journal, Vol. 6, No. 1, January 1968.

10. Ribich, W. A., and Richardson, H.H., "A Two Dimensional Fluid-Suspension Test Apparatus For Investigation of Pressure Ratio, Mach Number and Reynolds Number Effects," MIT Report No. PB-173-654.

Table 1 Values of η^*, g_1 and its derivatives as functions of the parameter r for $g_p = 1.000$

r	η	g_1	g_1'	g_1''	g_1'''
0.000000	0.000000	0.000000	0.000000	0.013889	0.000000
0.050000	0.600019	0.002500	0.008332	0.013880	-0.000043
0.100000	1.200300	0.010000	0.016650	0.013820	-0.000173
0.200000	2.404822	0.040000	0.033067	0.013337	-0.000680
0.300000	3.624682	0.090000	0.048650	0.012054	-0.001455
0.350000	4.246156	0.122500	0.055832	0.011014	-0.001896
0.400000	4.879741	0.160000	0.062400	0.009672	-0.002334
0.500000	6.202191	0.250000	0.072917	0.006076	-0.003080
0.560000	7.048856	0.313600	0.076943	0.003407	-0.003227
0.600000	7.645510	0.360000	0.078400	0.001481	-0.003207
0.630000	8.114793	0.396900	0.078745	0.000000	-0.003100
0.660100	8.608712	0.435732	0.078373	-0.001489	-0.002909
0.700100	9.309665	0.490140	0.076644	-0.003399	-0.002521
0.760100	10.492122	0.577752	0.071050	-0.005894	-0.001673
0.800100	11.407970	0.640160	0.065049	-0.007106	-0.000979
0.840100	12.482071	0.705768	0.056999	-0.007755	-0.000356
0.850100	12.734059	0.722670	0.054641	-0.007806	-0.000203
0.860100	13.105178	0.739772	0.052140	-0.007805	0.000084
0.880100	13.809656	0.774576	0.046689	-0.007634	0.000388
0.890100	14.201252	0.792278	0.043733	-0.007455	0.000520
0.930100	16.181313	0.865086	0.030288	-0.006020	0.000843
0.951100	17.697895	0.904591	0.022136	-0.004735	0.000826
0.964100	18.987557	0.929489	0.016692	-0.003729	0.000727
0.975100	20.495940	0.950820	0.011840	-0.002741	0.000581
0.988100	23.501902	0.976342	0.005810	-0.001401	0.000325
0.994100	26.332389	0.988235	0.002915	-0.000716	0.000173
0.995700	27.604160	0.991418	0.002132	-0.000526	0.000133
0.997000	29.049384	0.994009	0.001491	-0.000369	0.000091
0.997640	30.011752	0.995286	0.001174	-0.000292	0.000073
0.998412	31.599589	0.996827	0.000791	-0.000197	0.000049
0.998421	31.622359	0.996844	0.000787	-0.000196	0.000048
0.999861	41.348412	0.999722	0.000069	-0.000017	0.000004

Table 2 Calculated value of C_p and H/t for $\phi_1 = 60^\circ$

r	$\cos\phi_2$	C_{p_1}	C_p	H/t	ϕ_2
0.0500	0.735	3.000	1.200	0.825	43°
0.2001	0.575	1.650	0.905	1.310	55°
0.7601	0.440	0.910	0.610	2.060	64°
0.7300	0.340	0.540	0.426	3.100	70°
0.7001	0.230	0.272	0.230	5.400	76.67°
0.6800	0.175	0.140	0.133	9.600	80°

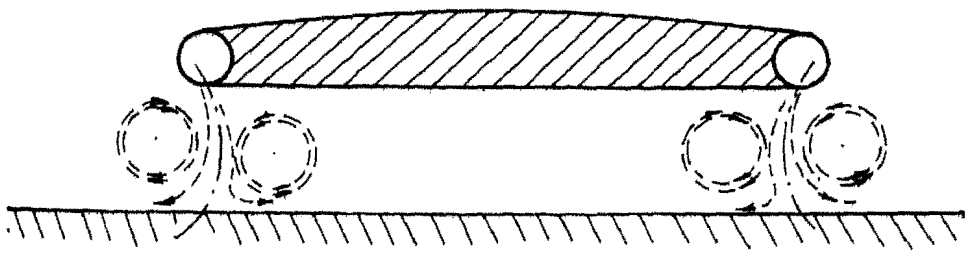

Fig. 1. Vortices Induced by Curtain Jet

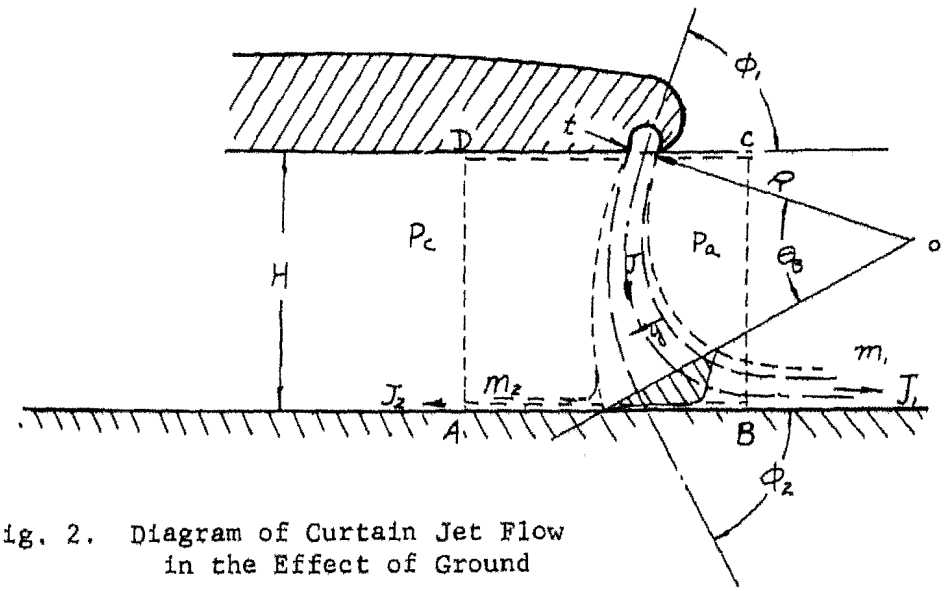

Fig. 2. Diagram of Curtain Jet Flow in the Effect of Ground

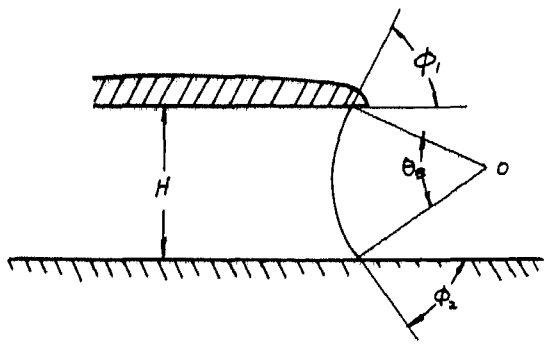

Fig. 3. Simplified Geometric Diagram of Curtain Jet

Fig. 4. Profiles of g and its derivatives (for g_∞ = 1.000).

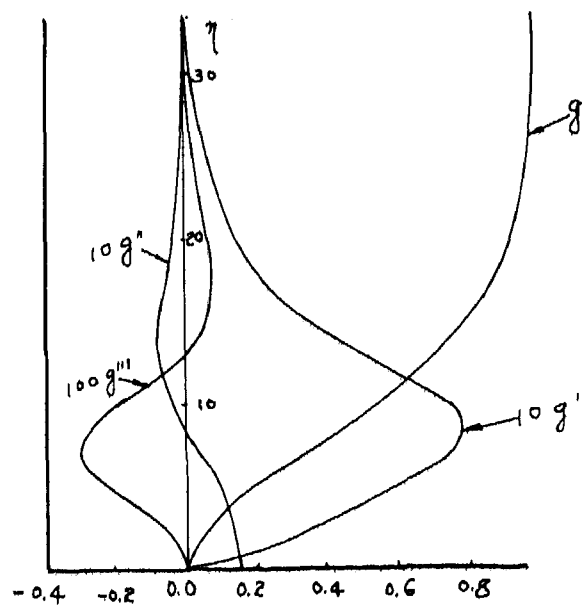

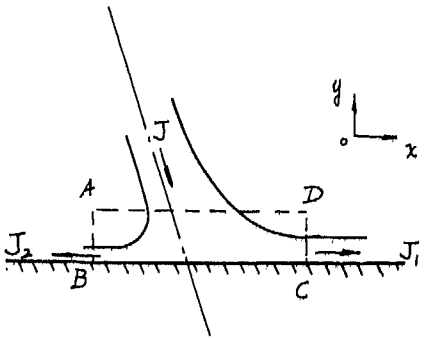

Fig. 5. Impingement of a Simple Jet on Ground

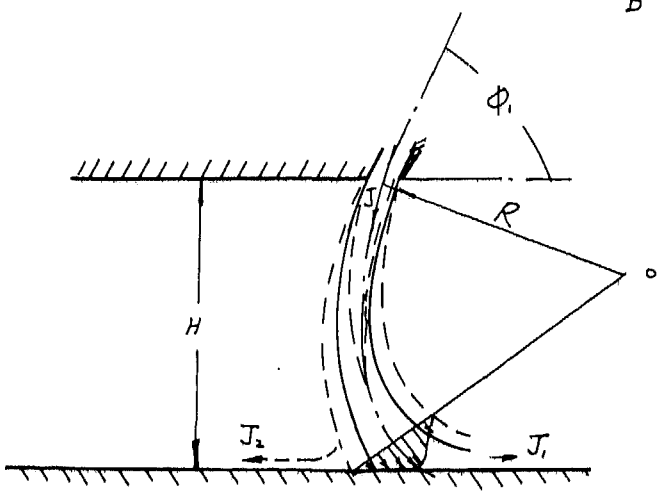

Fig. 6. Mixing region meet before jet impingement to provide fully developed jet shear flow at high (h/t) ratio.

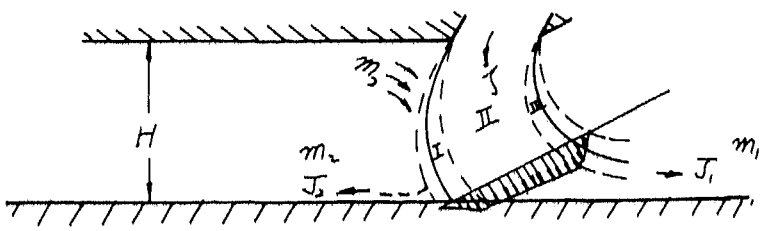

Fig. 7. Mixing region do not meet before jet impingement on ground at low (h/t) ratio.

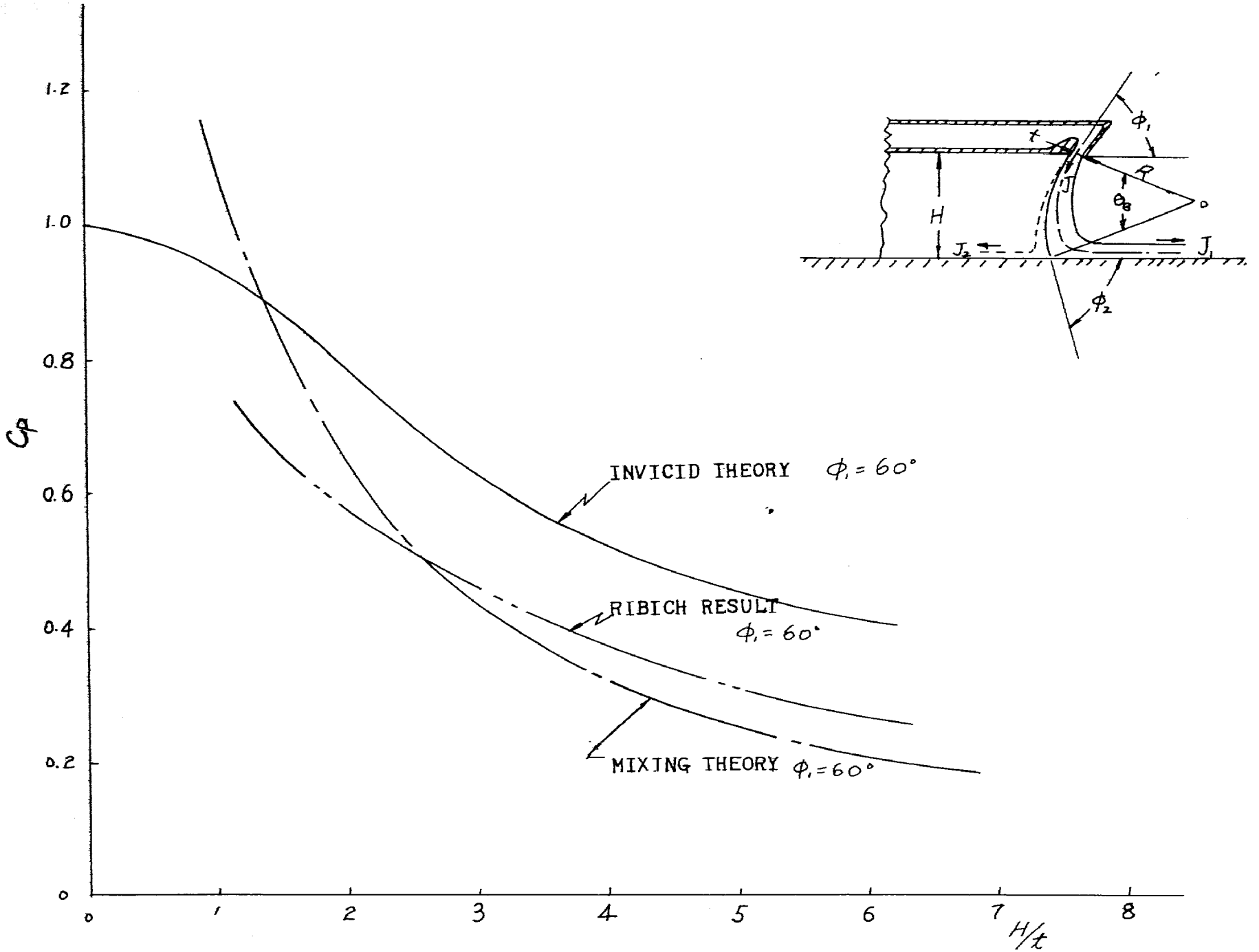

Fig. 8. Comparison of cushion pressure due to mixing, inviscid theory, and Ribich's result